



## **Mechanical behaviour of PEM fuel cell catalyst layers during regular cell operation**

**Maher A.R. Sadiq Al-Baghdadi**

Fuel Cell Research Center, International Energy & Environment Foundation, Al-Najaf, P.O.Box 39, Iraq.

### **Abstract**

Damage mechanisms in a proton exchange membrane fuel cell are accelerated by mechanical stresses arising during fuel cell assembly (bolt assembling), and the stresses arise during fuel cell running, because it consists of the materials with different thermal expansion and swelling coefficients. Therefore, in order to acquire a complete understanding of the mechanical behaviour of the catalyst layers during regular cell operation, mechanical response under steady-state hygro-thermal stresses should be studied under real cell operating conditions and in real cell geometry (three-dimensional). In this work, full three-dimensional, non-isothermal computational fluid dynamics model of a PEM fuel cell has been developed to investigate the behaviour of the cathode and anode catalyst layers during the cell operation. A unique feature of the present model is to incorporate the effect of hygro and thermal stresses into actual three-dimensional fuel cell model. In addition, the temperature and humidity dependent material properties are utilized in the simulation for the membrane. The model is shown to be able to understand the many interacting, complex electrochemical, transport phenomena, and deformation that have limited experimental data.

*Copyright © 2010 International Energy and Environment Foundation - All rights reserved.*

**Keywords:** Catalyst layers, PEM fuel cells, Durability, Hygro-thermal stress, CFD.

### **1. Introduction**

Escalating concerns regarding the impact that conventional methods of energy conversion are having on the environment and on global economics has in recent times progressively fuelled research and development into alternative technologies. One technology that is potentially independent of fossil fuels and suited to a wide range of applications from portable through to transport and stationary systems is the Polymer Electrolyte Membrane (PEM) Fuel Cell. PEM fuel cells have been the focus of significant research and development for over five decades. The electrochemical energy conversion device inherently mitigates the need to combust reactant gases directly which thereby prevents it from being restricted to the Carnot efficiency. PEM fuel cells operate on a hydrogen oxidation and oxygen reduction principal to generate electrical power and water as a bi-product. Single cells themselves can be 'stacked' to meet the power demands of the target application.

Each type of PEM fuel cell application will have its own set of requirements. During the course of research and development, this has resulted in a vast multitude of materials, designs, manufacturing techniques and considerations for the different components of the cell [1-3]. These variations also reflect the fact that there are indeed a multitude of factors that govern the performance of the PEM fuel cell, all

of which have some element of physical design or operation associated to it that can be altered to improve an aspect of cell performance.

Variations in operating modes and general cell design according to application means that how dominant certain performance degradation and failure mechanisms are also change according to application. Automotive fuel cells, for example, are likely to operate with neat hydrogen under loadfollowing or load-levelled modes and be expected to withstand variations in environmental conditions, particularly in the context of temperature and atmospheric composition. In addition, they are also required to survive over the course of their expected operational lifetimes i.e., around 5,500 hrs, while undergoing as many as 30,000 startup/shutdown cycles [4]. PEM fuel cells for stationary applications would not be subjected to as many startup/shutdown cycles, however, would be expected to survive up to 10,000 - 40,000 hrs of operation whilst maintaining a tolerance to fuel impurities in the reformat feed.

An important part of the fuel cell is the electrolyte, which gives every fuel cell its name. At the core of a PEM fuel cell is the polymer electrolyte membrane that separates the anode from the cathode. The desired characteristics of PEMs are high proton conductivity, good electronic insulation, good separation of fuel in the anode side from oxygen in the cathode side, high chemical and thermal stability, and low production cost. One type of PEMs that meets most of these requirements is Nafion. This is why Nafion is the most commonly used and investigated PEM in fuel cells.

In the Polymer-Electrolyte Membrane Fuel Cell the electrolyte consists of an acidic polymeric membrane that conducts protons but repels electrons, which have to travel through the outer circuit providing the electric work. A common electrolyte material is Nafion<sup>®</sup> from DuPont<sup>™</sup>, which consists of a fluoro-carbon backbone, similar to Teflon, with attached sulfonic acid groups. The membrane is characterized by the fixed-charge concentration (the acidic groups): the higher the concentration of fixed-charges, the higher is the protonic conductivity of the membrane. Alternatively, the term "equivalent weight" is used to express the mass of electrolyte per unit charge.

For optimum fuel cell performance it is crucial to keep the membrane fully humidified at all times, since the conductivity depends directly on water content. The thickness of the membrane is also important, since a thinner membrane reduces the ohmic losses in a cell. However, if the membrane is too thin, hydrogen, which is much more diffusive than oxygen, will be allowed to cross-over to the cathode side and recombine with the oxygen without providing electrons for the external circuit.

The best catalyst material for both anode and cathode PEM fuel cell is platinum. Since the catalytic activity occurs on the surface of the platinum particles, it is desirable to maximize the surface area of the platinum particles. A common procedure for surface maximization is to deposit the platinum particles on larger carbon black particles.

Therefore, the catalyst is characterized by the surface area of platinum by mass of carbon support. The electrochemical half-cell reactions can only occur, where all the necessary reactants have access to the catalyst surface. This means that the carbon particles have to be mixed with some electrolyte material in order to ensure that the hydrogen protons can migrate towards the catalyst surface. This "coating" of electrolyte must be sufficiently thin to allow the reactant gases to dissolve and diffuse towards the catalyst surface. Since the electrons travel through the solid matrix of the electrodes, these have to be connected to the catalyst material, i.e. an isolated carbon particle with platinum surrounded by electrolyte material will not contribute to the chemical reaction.

Several methods of applying the catalyst layer to the gas diffusion electrode have been reported. These methods are spreading, spraying, and catalyst power deposition. For the spreading method, a mixture of carbon support catalyst and electrolyte is spread on the GDL surface by rolling a metal cylinder on its surface. In the spraying method, the catalyst and electrolyte mixture is repeatedly sprayed onto the GDL surface until a desired thickness is achieved. Although the catalyst layer thickness can be up to 50  $\mu\text{m}$  thick, it has been found that almost all of the electrochemical reaction occurs in a 10  $\mu\text{m}$  thick layer closest to the membrane.

In order to maximise the electrochemically active surface area (EASA) in the anodic and cathodic catalyst layers, the catalyst is applied as fine and widely dispersed nano-particles on the surface of a supporting particle [5]. Typically, the catalyst is platinum or platinum alloyed with ruthenium or chromium for example, and the larger supporting particle is commonly carbon-based. Recent studies have shown that within 2000 hrs of operation, it is possible for the metal catalyst to undergo morphological change, in the form of catalytic agglomeration and/or ripening [6]. This leads on to a gradual decrease in the EASA. Whilst agglomeration is observed for both anode and cathode catalyst

layers, it is usually the cathodic particles that undergo more extensive agglomeration, where there is an increased presence of liquid water and which facilitates primary corrosion [7]. Repetitive on/off load cycles for PEM fuel cells can also cause platinum sintering; residual hydrogen can induce a high voltage equivalent to open-circuit voltage to the cathode, causing the sintering to occur [8]. This can be mitigated by air-purging the anode channel.

Another mechanism for the loss of EASA could be attributed to the movement of platinum. When the PEM fuel cell is operated through hydrogen-air open circuit to air-air open circuit, platinum can become quite soluble and consequently liable to transportation through adjacent layers [9]. Loss of platinum correspondingly compromises the EASA. Such phenomenon can also be accompanied by an apparent migration of platinum. Migration of metal catalyst particles in both the anode and cathode catalyst layers in PEM fuel cells has been observed, moving towards the interface between the catalyst layer and the membrane [8].

Mechanical stresses which limit MEA durability have two origins. Firstly, this is the stresses arising during fuel cell assembly (bolt assembling). The bolts provide the tightness and the electrical conductivity between the contact elements. Secondly, additional mechanical stresses occur during fuel cell running because PEM fuel cell components have different thermal expansion and swelling coefficients. Thermal and humidity gradients in the fuel cell produce dilatations obstructed by tightening of the screw-bolts. Compressive stress increasing with the hygro-thermal loading can exceed the yield strength which causes the plastic deformation. The mechanical behaviour of the membrane depends strongly on hydration and temperature [10, 11]. Due to water management issues, operating conditions need to be carefully chosen in order to properly operate fuel cells. Because of the gas consumption along the feeding channels and water production at the cathode, internal cell humidification is highly inhomogeneous. Consequently, operating fuel cells are very often close to critical operating conditions, such as flooding and drying, at least locally [12].

An operating fuel cell has varying local conditions of temperature, humidity, and power generation (and thereby heat generation) across the active area of the fuel cell in three-dimensions. Nevertheless, except of ref. [11], no models have yet been published to incorporate the effect of hygro-thermal stresses into actual fuel cell models to study the effect of these real conditions on the stresses developed in membrane and gas diffusion layers. In addition, as a result of the architecture of a cell, the transport phenomena in a fuel cell are inherently three-dimensional, but no models have yet been published to address the hygro-thermal stresses in PEM fuel cells with three-dimensional effect. Suvorov et al. [13] reported that the error introduced due to two-dimensional assumption is about 10%. Therefore, in order to acquire a complete understanding of the mechanical behaviour of the catalyst layers during regular cell operation, mechanical response under steady-state hygro-thermal stresses should be studied under real cell operating conditions and in real cell geometry (three-dimensional).

## 2. Model description

Assuming linear response within the elastic region, the isotropic Hooke's law is used to determine the stress tensor.

$$\sigma = \mathbf{D}\varepsilon \quad (1)$$

where  $\sigma$  is the stress (Pa),  $\varepsilon$  is the strain, and  $\mathbf{D}$  is the constitutive matrix.

Using hygrothermoelasticity theory, the effects of temperature and moisture as well as the mechanical forces on the behaviour of elastic bodies have been addressed. An uncoupled theory is assumed. The total strain tensor in membrane ( $\varepsilon_{mem}$ ) is determined using the following expression;

$$\varepsilon_{mem} = \varepsilon_M + \varepsilon_T + \varepsilon_S \quad (2)$$

where,  $\varepsilon_M$  is the contribution from the mechanical forces and  $\varepsilon_T$ ,  $\varepsilon_S$  are the thermal and swelling induced strains, respectively.

The thermal strains resulting from a change in temperature of an unconstrained isotropic volume are given by;

$$\varepsilon_T = \alpha(T - T_{Ref}) \quad (3)$$

where  $\alpha$  is membrane thermal expansion (1/K), and  $T$  is local temperature (K).

Similarly, the swelling strains caused by moisture change are given by;

$$\varepsilon_S = \beta_{mem}(\mathfrak{R} - \mathfrak{R}_{Ref}) \quad (4)$$

where  $\beta_{mem}$  is the membrane swelling coefficient tensor due to moisture absorption (1/%), and  $\mathfrak{R}$  is relative humidity (%).

Following the work [14], the swelling-expansion for the membrane,  $\beta_{mem}$ , is expressed as a polynomial function of humidity and temperature as follows;

$$\beta_{mem} = \sum_{i,j=1}^4 C_{ij} T^{4-i} \mathfrak{R}^{4-j} \quad (5)$$

where  $C_{ij}$  is the polynomial constants, see Ref. [14].

The geometric and the base case operating conditions are listed in Table 1. Values of the electrochemical transport parameters for the base case operating conditions are taken from reference [11] and are listed in Table 2. The material properties for the fuel cell components used in this model are taken from reference [14] and are shown in Tables 3-5.

The mechanical boundary conditions are noted in Figure 1. The initial conditions corresponding to zero stress-state are defined; all components of the cell stack are set to reference temperature 20 C, and relative humidity 35% (corresponding to the assembly conditions). In addition, a constant pressure of (1 MPa) is applied on the surface of lower graphite plate, corresponding to a case where the fuel cell stack is equipped with springs to control the clamping force.

This stress model has been incorporated into full three-dimensional, multi-phase, non-isothermal computational fluid dynamics model of a proton exchange membrane fuel cell. The three-dimensional CFD model of a PEM fuel cell that used with the present stress model was developed, validated, and discussed in detail by the current author in his previous paper [11]. In brief, the model is based on the computational fluid dynamics method and considers multi-phase, multi-component flow inside the gas flow channels and the porous media of a PEM fuel cell with straight flow channels. The full computational domain consists of cathode and anode gas flow channels, and the membrane electrode assembly as shown in Figure 1. The model accounts for both gas and liquid phase in the same computational domain, and thus allows for the implementation of phase change inside the gas diffusion layers. The model includes the transport of gaseous species, liquid water, protons, energy, and water dissolved in the ion-conducting polymer. Water transport inside the porous gas diffusion layer and catalyst layer is described by two physical mechanisms: viscous drag and capillary pressure forces, and is described by advection within the gas channels. Water transport across the membrane is also described by two physical mechanisms: electro-osmotic drag and diffusion. Water is assumed to be exchanged among three phases; liquid, vapour, and dissolved, and equilibrium among these phases is assumed. This model takes into account convection and diffusion of different species in the channels as well as in the porous gas diffusion layer, heat transfer in the solids as well as in the gases, and electrochemical reactions. The model reflects the influence of the operating parameters on fuel cell performance to investigate the in situ total displacement and degree of the deformation of the polymer membrane of PEM fuel cells.

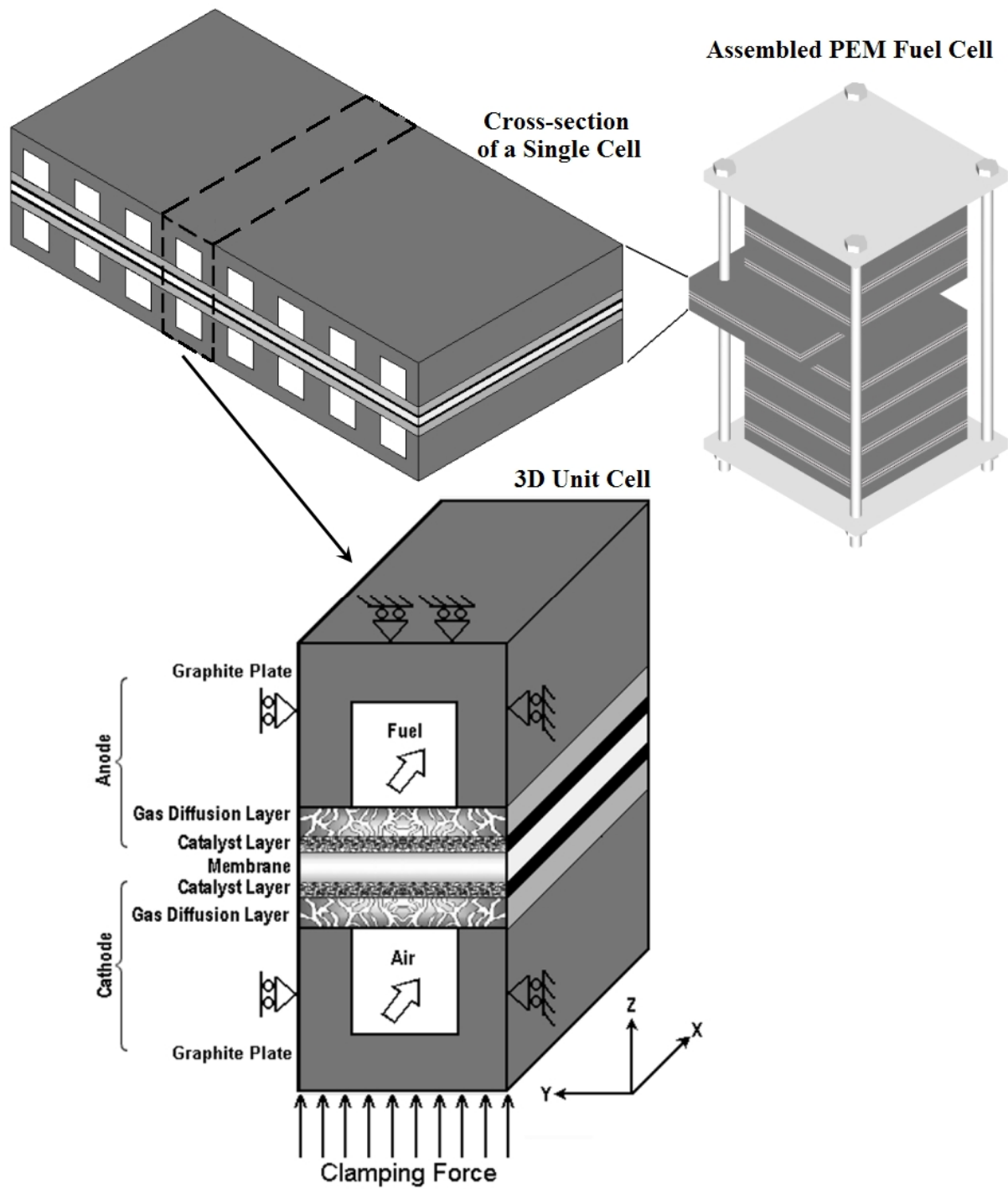


Figure 1. Three-dimensional computational domain

Table 1. Geometrical and operational parameters for base case conditions

Parameter	Symbol	Value	Unit
Channel length	$L$	0.05	$m$
Channel width	$W$	1e-3	$m$
Channel height	$H$	1e-3	$m$
Land area width	$W_{land}$	1e-3	$m$
Gas diffusion layer thickness	$\delta_{GDL}$	0.26e-3	$m$
Wet membrane thickness (Nafion® 117)	$\delta_{mem}$	0.23e-3	$m$
Catalyst layer thickness	$\delta_{CL}$	0.0287e-3	$m$
Hydrogen reference mole fraction	$x_{H_2}^{ref}$	0.84639	-
Oxygen reference mole fraction	$x_{O_2}^{ref}$	0.17774	-
Anode pressure	$P_a$	3	$atm$
Cathode pressure	$P_c$	3	$atm$
Inlet fuel and air temperature	$T_{cell}$	353.15	$K$
Relative humidity of inlet fuel and air (fully humidified conditions)	$\psi$	100	%
Air stoichiometric flow ratio	$\xi_c$	2	-
Fuel stoichiometric flow ratio	$\xi_a$	2	-

Table 2. Electrode and membrane parameters for base case operating conditions

Parameter	Symbol	Value	Unit
Electrode porosity	$\varepsilon$	0.4	-
Electrode electronic conductivity	$\lambda_e$	100	$S/m$
Membrane ionic conductivity (Nafion® 117)	$\lambda_m$	17.1223	$S/m$
Transfer coefficient, anode side	$\alpha_a$	0.5	-
Transfer coefficient, cathode side	$\alpha_c$	1	-
Cathode reference exchange current density	$i_{o,c}^{ref}$	1.8081e-3	$A/m^2$
Anode reference exchange current density	$i_{o,a}^{ref}$	2465.598	$A/m^2$
Electrode thermal conductivity	$k_{eff}$	1.3	$W/m.K$
Membrane thermal conductivity	$k_{mem}$	0.455	$W/m.K$
Electrode hydraulic permeability	$kp$	1.76e-11	$m^2$
Entropy change of cathode side reaction	$\Delta S$	-326.36	$J/mole.K$
Heat transfer coefficient between solid and gas phase	$\beta$	4e6	$W/m^3$
Protonic diffusion coefficient	$D_{H^+}$	4.5e-9	$m^2/s$
Fixed-charge concentration	$c_f$	1200	$mole/m^3$
Fixed-site charge	$z_f$	-1	-
Electro-osmotic drag coefficient	$n_d$	2.5	-

Table 3. Material properties used in the model

Parameter	Symbol	Value	Unit
Electrode Poisson's ratio	$\mathfrak{S}_{GDL}$	0.25	-
Membrane Poisson's ratio	$\mathfrak{S}_{mem}$	0.25	-
Electrode thermal expansion	$\alpha_{GDL}$	-0.8e-6	1/K
Membrane thermal expansion	$\alpha_{mem}$	123e-6	1/K
Electrode Young's modulus	$\Psi_{GDL}$	1e10	Pa
Membrane Young's modulus	$\Psi_{mem}$	Table 4	Pa
Electrode density	$\rho_{GDL}$	400	kg/m <sup>3</sup>
Membrane density	$\rho_{mem}$	2000	kg/m <sup>3</sup>
Membrane humidity swelling-expansion tensor	$\beta_{mem}$	from eq.(2)	1/%

Table 4. Young's modulus at various temperatures and humidities of Nafion

Young's modulus [MPa]	Relative humidity [%]			
	30	50	70	90
T=25 C	197	192	132	121
T=45 C	161	137	103	70
T=65 C	148	117	92	63
T=85 C	121	85	59	46

Table 5. Yield strength at various temperatures and humidities of Nafion

Yield stress [MPa]	Relative humidity [%]			
	30	50	70	90
T=25 C	6.60	6.14	5.59	4.14
T=45 C	6.51	5.21	4.58	3.44
T=65 C	5.65	5.00	4.16	3.07
T=85 C	4.20	3.32	2.97	2.29

### 3. Results and discussion

Results for the cell operates at nominal current density of 1.4 A/cm<sup>2</sup> are discussed in this section. The selection of relatively high current density is due to illustrate the phase change effects, where it becomes clearly apparent between single and multi-phase model in the mass transport limited region.

Thermal management is required to remove the heat produced by the electrochemical reaction in order to prevent drying out of the membrane and excessive thermal stresses that may result in rupture of the membrane or mechanical damage in the cell. The small temperature differential between the fuel cell stack and the operating environment make thermal management a challenging problem in PEM fuel cells. The temperature distribution inside the fuel cell has important effects on nearly all transport phenomena, and knowledge of the magnitude of temperature increases due to irreversibilities might help preventing cell failure.

Figure 2 shows the distribution of the temperature at the cathode and anode catalyst layers at a nominal current density of 1.4 A/cm<sup>2</sup>. In general, the temperature at the cathode side is higher than at the anode

side, due to the reversible and irreversible entropy production. Naturally, the maximum temperature occurs, where the electrochemical activity is highest, which is near the cathode side inlet area. The temperature peak appears in the cathode catalyst layer, implying that major heat generation takes place in this region.

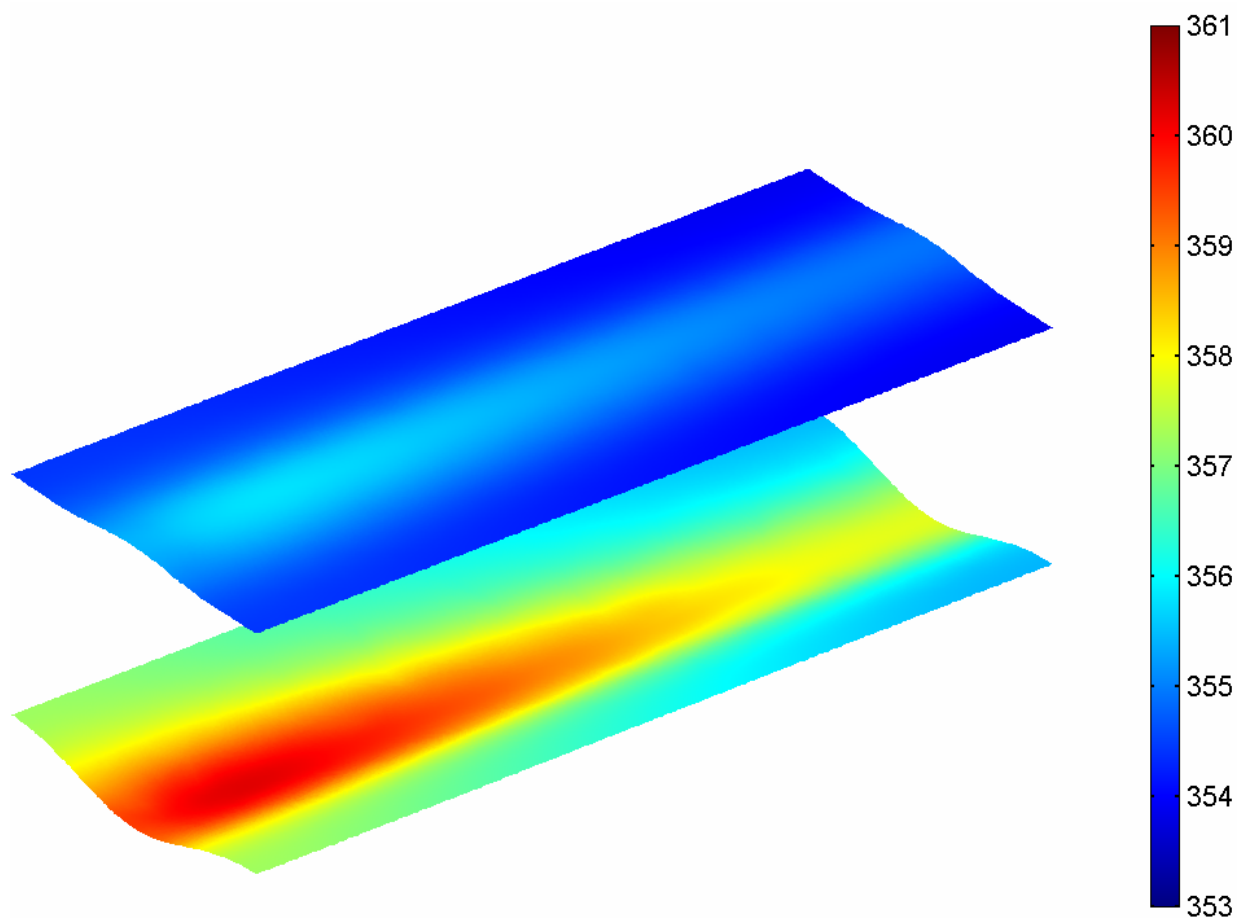


Figure 2. Temperature [K] distribution at the cathode (lower) and anode (upper) catalyst layers (deformed shape plot, scale enlarged 500 times)

The durability of proton exchange membranes used in fuel cells is a major factor in the operating lifetime of fuel cell systems. Figure 3 shows the total displacement distribution at the upper and lower surface of the cell membrane, i.e. at the catalyst layers, at a nominal current density of  $1.4 \text{ A/cm}^2$ . The figure illustrates the effect of stresses on the catalyst layers. Because of the different thermal expansion and swelling coefficients between gas diffusion layers, membrane, and catalyst layers materials with non-uniform temperature distributions in the cell during operation, hygro-thermal stresses and deformation are introduced. The non-uniform distribution of stress, caused by the temperature gradient in the cell, induces localized bending stresses, which can contribute to delaminating between the membrane, catalyst layers, and the gas diffusion layers. The non-uniform distribution of stresses can also contribute to delaminating between the gas diffusion layers and the bipolar plates. These stresses may explain the occurrence of cracks and pinholes in the fuel cells membranes under steady-state loading during regular cell operation, especially in the high loading conditions. In addition, it was found from Figure 3 that the stresses and then decay of the catalyst is more serious than that of the PEM.

The model result (Figure 3) is conforming to experimental data provided by Luo et al. [15]. The results of Luo et al. [15] show the surface SEM micrograph of the original PEMs and the degraded PEMs at the catalyst layer. It is clearly that the original PEMs are surface compact while there are many of crackles on the surface of the degraded PEMs. It is reported in the former literature that many of the mechanical life failures result from cracking, tearing and puncture of the PEMs. In the study of Luo et al. [15], the formation of punctures, which is generally considered resulting from introduction of the foreign particles

or fibers during the MEA fabrication process that might perforate the PEM, have not been observed. The formation of the crackles most likely come from the constantly switchover of the humidification and the highest mechanical stresses close to the sealing and electrode/membrane edges.

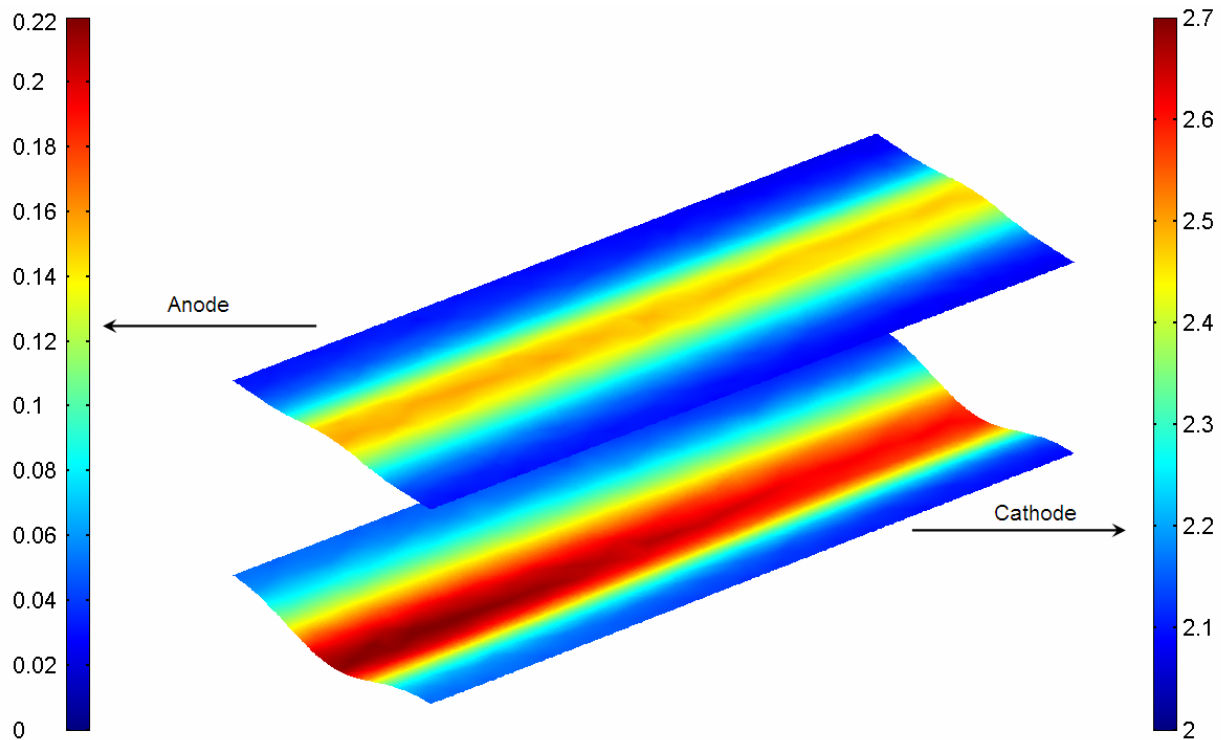


Figure 3. Total displacement [ $\mu\text{m}$ ] distributions in the membrane along the lower (cathode) and upper (anode) surfaces of the membrane at base case conditions (deformed shape plot, scale enlarged 500 times)

#### 4. Conclusion

Full three-dimensional, non-isothermal computational fluid dynamics model of a PEM fuel cell has been developed to investigate the behaviour of the cathode and anode catalyst layers during the cell operation. A unique feature of the present model is to incorporate the effect of hygro and thermal stresses into actual three-dimensional fuel cell model. In addition, the temperature and humidity dependent material properties are utilized in the simulation for the membrane. The model is shown to be able to understand the many interacting, complex electrochemical, transport phenomena, and deformation that have limited experimental data. The model is shown to be able to: (1) understand the many interacting, complex electrochemical, transport phenomena, and deformation, which, cannot be studied experimentally; (2) identify limiting steps and components; and (3) provide a computer-aided tool for design and optimization of future fuel cell with much higher power density and lower cost. The results show that the non-uniform distribution of stresses, caused by the temperature gradient in the cell, induces localized bending stresses, which can contribute to delaminating between the membrane and the gas diffusion layers. These stresses may explain the occurrence of cracks and pinholes in the membrane under steady-state loading during regular cell operation. It was also found that the stresses and then decay of the catalyst is more serious than that of the PEM.

#### References

- [1] Mehta V, Cooper JS. Review and analysis of PEM fuel cell design and manufacturing. *Journal of Power Sources* 2003; 114:32-53.
- [2] Haile SM. Fuel cell materials and components. *Acta Materialia* 2003; 51:5981-6000.

- [3] Cooper JS. Design analysis of PEMFC bipolar plates considering stack manufacturing and environmental impact. *Journal of Power Sources* 2004; 129:152-169.
- [4] Yu PT, Gu W, Makharia R, Wagner FT, Gasteiger A. The Impact of Carbon Stability on PEM Fuel Cell Startup and Shutdown Voltage Degradation. 210th ECS Meeting, Cancun, Mexico, Durability – Fuel Starvation and Start/Stop Degradation, October 29-November 3 2006.
- [5] Larminie J, Dicks A. *Fuel Cell Systems Explained*, Second Edition. John Wiley & Sons 2003. Chichester.
- [6] Xie J, Wood III DL, Wayne DM, Zawodzinski TA, Atanassov P, Borup RL. Durability of PEFCs at High Humidity Conditions. *Journal of The Electrochemical Society* 2005; 152(1):A104-A113.
- [7] Xie J, Wood III DL, More KL, Atanassov P, Borup RL. Microstructural Changes of membrane Electrode Assemblies during PEFC Durability Testing at High Humidity Conditions. *Journal of The Electrochemical Society* 2005; 152(5):A1011-A1020.
- [8] Lee S-Y, Cho E, Lee J-H, Kim H-J, Lim T-H, Oh I-H, Won J. Effects of Purging on the Degradation of PEMFCs Operating with Repetitive On/Off Cycles. *Journal of The Electrochemical Society* 2007; 154(2):B194-B200.
- [9] Darling RM, Meyers JP. Mathematical Model of Platinum Movement in PEM Fuel Cells. *Journal of The Electrochemical Society* 2005; 152(1):A242-A247.
- [10] Maher A.R. Sadiq Al-Baghdadi. A CFD study of hygro-thermal stresses distribution in tubular-shaped ambient air-breathing PEM micro fuel cell during regular cell operation. *International Journal of Energy and Environment IJEE*, 2010; 1(2): 183-198.
- [11] Maher A.R. Sadiq Al-Baghdadi. Modeling optimizes PEM fuel cell durability using three-dimensional multi-phase computational fluid dynamics model. *International Journal of Energy and Environment IJEE*, 2010; 1(3): 375-398.
- [12] F. Brèque, J. Ramousse, Y. Dubé, K. Agbossou, P. Adzakpa. Sensibility study of flooding and drying issues to the operating conditions in PEM Fuel Cells. *International Journal of Energy and Environment IJEE*, 2010; 1(1):1-20.
- [13] Suvorov, A.P.; Elter, J.; Staudt, R.; Hamm, R.; Tudryn, G.J.; Schadler, L.; Eisman, G. Stress relaxation of PBI based membrane electrode assemblies. *Int. J. Solids and Structures*, 2008; 45(24): 5987-6000.
- [14] Kusoglu A., Karlsson A.M., Santare M.H., Cleghorn S., Johnson W.B. Mechanical response of fuel cell membranes subjected to a hygro-thermal cycle. *J. Power Sources*, 2006; 161(2): 987-996.
- [15] Z. Luo, D. Li, H. Tang, M. Pan, R. Ruan. Degradation behavior of membrane–electrode-assembly materials in 10-cell PEMFC stack. *International Journal of Hydrogen Energy*, 2006; 31: 1831-1837.